

A computer investigation of chemically mediated detachment in bacterial biofilms

Stephen M. Hunt, Martin A. Hamilton, John T. Sears, Gary Harkin and Jason Reno

Center for Biofilm Engineering, Montana State University, Bozeman, MT 59717-3980, USA

Correspondence

Stephen M. Hunt
steve_h@erc.montana.edu

Received 19 November 2002

Revised 22 January 2003

Accepted 23 January 2003

A three-dimensional computer model was used to evaluate the effect of chemically mediated detachment on biofilm development in a negligible-shear environment. The model, BacLAB, combines conventional diffusion-reaction equations for chemicals with a cellular automata algorithm to simulate bacterial growth, movement and detachment. BacLAB simulates the life cycle of a bacterial biofilm from its initial colonization of a surface to the development of a mature biofilm with cell areal densities comparable to those in the laboratory. A base model founded on well established transport equations that are easily adaptable to investigate conjectures at the biological level has been created. In this study, the conjecture of a detachment mechanism involving a bacterially produced chemical detachment factor in which high local concentrations of this detachment factor cause the bacteria to detach from the biofilm was examined. The results show that the often observed 'mushroom'-shaped structure can occur if detachment events create voids so that the remaining attached cells look like mushrooms.

INTRODUCTION

That multicellular biofilms on surfaces may be the predominant state of bacteria in the natural environment is gaining widespread acceptance. According to Watnick (2000), if taken to the extreme, we may view the planktonic, or free-swimming, phase primarily as a mechanism for translocating from one surface to another. For bacteria to avoid density-mediated starvation and to colonize new surfaces, cells must be able to leave the biofilm and disperse. This process of cell transfer from a mature biofilm to an unoccupied surface is a plausible strategy for the long-term survival of bacteria. The mode by which cells detach is, therefore, a critical stage in the life cycle of biofilms (Sauer *et al.*, 2002).

It is known that biofilms are heterogeneous structures from which both single cells and multicellular aggregates slough (Stewart *et al.*, 1994). It has been suggested that freely diffusible chemical signals play an important role in biofilm development and maintenance (Davies *et al.*, 1998; Kolter *et al.*, 1998). Although the mechanisms have not been established, there is some experimental evidence that a subset of these chemical signals plays an active role in biofilm detachment (Allison *et al.*, 1999; Boyd & Chakrabarty, 1994). Boyd & Chakrabarty (1994) state that when expressed from a regulated promoter, alginate lyase can induce enhanced sloughing of cells due to degradation of the alginate.

Mathematical models have been used for the last three decades to synthesize and integrate our knowledge about the behaviour of microbial biofilms. Early models represented biofilms as homogeneous steady-state films containing a single species (Rittmann & McCarty, 1980). They later evolved to dynamic multisubstrate-multispecies biofilm computer models (Rittmann & Manem, 1992; Wanner & Gujer, 1986; Wanner & Reichert, 1996). Although these models were advanced descriptions, they were governed exclusively by one-dimensional mass transport and biochemical interactions and the models could not account for the experimentally observed three-dimensional heterogeneity resulting from bacterial attachment, growth and detachment. The morphology was essentially predetermined by the modeller. Detachment was represented by an arbitrary uniform removal rate or velocity. These models are generally suitable for representing aggregate biofilm activity on many square millimetres of surface area.

The subsequent generation of biofilm models focused on a smaller scale. Most utilized discrete methods, such as cellular automata, to simulate the rules that govern the lives of microbial cells. These models produced realistic, structurally heterogeneous biofilms (Barker & Grimson, 1993; Colasanti, 1992; Eberl *et al.*, 2000; Ermentrout & Edelstein-Keshet, 1993; Hermanowicz, 1998, 1999; Kreft *et al.*, 1998; Noguera *et al.*, 1999; Picioreanu *et al.*, 1998; Wimpenny & Colasanti, 1997). They allowed the artificial biofilm structure to evolve as a self-organization process, emulating how bacterial cells organize themselves into biofilms. Some models ignored detachment, while others viewed detachment as a process completely dependent on

An example animation from a single simulation using the BacLAB computer model is available as supplementary data in *Microbiology* Online (<http://mic.sgmjournals.org>).

the shear-stress induced by the flowing bulk liquid. No published models consider other potential detachment mechanisms.

The aim of this article is to evaluate the implications of a chemically mediated detachment mechanism through computer experimentation. We describe a three-dimensional biofilm model that combines conventional diffusion-reaction equations for chemicals to model solute transport and a cellular automata algorithm to simulate the bacterial growth, movement and detachment. Three different plausible cellular automata detachment rules are examined by conducting 20 replicate simulations for each detachment rule. Detachment via a hypothetical bacterially produced chemical detachment factor produces structures compatible with the known morphology and dynamic behaviour of biofilms. We conclude that the simulation results are both qualitatively and quantitatively similar to those for laboratory biofilms. The conjecture of a chemically mediated detachment mechanism is not invalidated.

MODEL DESCRIPTION

The present computer model, named BacLAB, describes the dynamic, stochastic behaviour of a bacterial biofilm on a surface (substratum) in an aqueous environment. Although the bulk liquid is assumed to be well-mixed, it produces no shear-stress on the biofilm. BacLAB blends a conventional, deterministic differential equations model for chemical reaction and diffusion with a stochastic cellular automata model for bacterial cell division, detachment and movement. The scale of the modelling domain, approximately 1 mm², is suitable for describing the local environment of an individual bacterium in a biofilm colony. The unique feature of BacLAB is its ability to include a chemical factor, produced by the bacteria, which leads to detachment when large local concentrations are achieved. The existence of such a detachment factor is an important conjecture (Potera, 1999), the implications of which are conveniently explored by computer experimentation with this model.

The domain. The spatial domain, Γ , of the model consists of a box, typically 900 μm per side, containing two overlapping computational grids. The first grid is a fixed lattice used to represent any soluble components (e.g. substrate, detachment factor) in the model. The second grid partitions the model space into many small cubes, each cube being a volume element large enough (here assumed 3 μm per side) to include a bacterial cell and its associated extracellular polymeric substance (Characklis, 1989). Coordinates of each cube and lattice point are then uniquely given by the set of vectors $\{(x,y,z)$ such that $x=0\dots N_x-1$, $y=0\dots N_y-1$, $z=0\dots N_z-1\}$. There are $N_x \cdot N_y \cdot N_z$ total lattice points and cubes. In our simulations $N_x=N_y=N_z=300$. Here $z=0$ indicates an element on the substratum, and $z=N_z-1$ indicates an element the furthest from the substratum. There is a one-to-one correspondence between lattice points and cubes.

The temporal domain is discrete with equally spaced time points, typically 1 h apart, chosen to be small with respect to biofilm development.

State variables. At any time point, three primary arrays are used to represent the state of the system: $S=\{C_S(x,y,z)\}$, $F=\{C_F(x,y,z)\}$ and $B=\{B(x,y,z)\}$, where $C_S(x,y,z)$ denotes the concentration of the limiting substrate, $C_F(x,y,z)$ denotes the concentration of the detachment factor and $B(x,y,z)$ denotes the occupation state at location (x,y,z) .

Each element within the substrate and detachment arrays, $C_S(x,y,z)$ and $C_F(x,y,z)$, contains a positive real value corresponding to that solute's concentration at that node location. The occupation state of a cube, $B(x,y,z)$, is represented by an identity pointer to a vector, $I_{\text{bacterium}}$, containing all relevant information (e.g. bacterial species, kinetic parameters, etc.) about an individual bacterium. If the cube is unoccupied by a bacterium, it is represented by a null identity pointer. When computing the state of the system at the next time point, S and F are updated using conventional differential equations, while B is updated using cellular automata rules.

Differential equations for solutes. In the aqueous environment being modelled, the bulk liquid is well-mixed, but imposes no shear-stress on the biofilm. The solutes are transported solely by diffusion in the biofilm. The concentrations $C_S(x,y,z)$ and $C_F(x,y,z)$ are a result of molecular diffusion and reaction (consumption or production) with the bacteria. The diffusional time constant is approximately 100 orders of magnitude smaller than that for bacterial cell division (Picioreanu, 1999). Thus, molecular diffusion can be assumed to be at steady-state with respect to the bacterial growth. Suppressing the location indices (x,y,z) , let C_i denote the concentration of solute i , where i is either the limiting substrate, S , or the chemical detachment factor, F . Let the parameter D_i denote the diffusivity coefficient of solute i . The diffusivity in the biofilm is calculated by multiplying the diffusivity of the solute in the aqueous or bulk phase, $D_{i,\text{aq}}$, by the relative effective diffusivity, $D_{i,e}/D_{i,\text{aq}}$. The variable X denotes the biomass density (calculated as average cell mass per cube volume for occupied cubes and 0 otherwise), and $r_i(C_S,X)$ denotes the reaction term (to be defined below) corresponding to substrate i 's consumption or production by the bacteria. A negative r_i value indicates substrate conversion into biomass and a positive r_i value indicates that the bacteria are producing the solute, as is the case for the chemical detachment factor. Equation (1) is the three-dimensional representation for diffusive transport and reaction.

$$0 = D_i \left(\frac{\partial^2 C_i}{\partial x^2} + \frac{\partial^2 C_i}{\partial y^2} + \frac{\partial^2 C_i}{\partial z^2} \right) + r_i(C_S, X) \quad (1)$$

Equation (2) is the classical Monod (1949) equation for the substrate consumption by bacteria. Here μ_{max} denotes the maximum specific growth rate, Y_{XS} denotes the yield

coefficient and K_s denotes the half-saturation coefficient.

$$r_S(C_S, X) = \left(\frac{\mu_{\max} \cdot X}{Y_{XS}} \right) \left(\frac{C_S}{K_s + C_S} \right) \quad (2)$$

Using small time steps, Δt , relative to growth, we approximate the reaction term by calculating the reaction rate at the current time step, t . Using finite differences to approximate the derivative in Equation (1), the result is a three-dimensional block tridiagonal linear system. This system is then solved using a discrete fast Fourier transform for the concentration at $t + \Delta t$. The solver used was the `pois3d` subroutine from the FISHPACK library (available at <http://www.netlib.org/fishpack/>).

Let the parameter k denote the detachment factor production coefficient. Equation (3) is an assumed first order kinetic expression in C_S for the detachment factor production. This first order expression in C_S attempts to correlate the detachment factor production with cellular activity. It is therefore assumed that, when a cell is in a starved state, energy is conserved and extra cellular chemicals are not actively produced.

$$r_F(C_S, X) = \begin{cases} 0, & \text{if } B = \text{Null Identity Pointer} \\ k \cdot C_S, & \text{if } B \neq \text{Null Identity Pointer} \end{cases} \quad (3)$$

Equation (3), inserted into (1) for r_i , where C_i is the detachment factor concentration, C_F , again results in a three-dimensional block tridiagonal linear system and can be solved as indicated above.

The model's substrate uptake from the surrounding environment is dictated by the set of boundary conditions used in the simulation. The substratum is modelled as an impermeable surface by specifying a no flux boundary condition at $z=0$.

$$\left. \frac{dC_i}{dz} \right|_{z=0} = 0 \quad \text{for } i = S, F \quad (4)$$

The substrate source is generated by maintaining a constant concentration of the substrate in the bulk fluid, $C_{S,\text{bulk}}$, at a fixed height above the top of the biofilm as a moving boundary. Conversely, a sink for the detachment factor is created by maintaining the concentration in the bulk fluid at zero, i.e. $C_{F,\text{bulk}} = 0$. This feature is reasonable if convective transport removes the detachment factor from locations in the bulk liquid above the top of the biofilm.

To eliminate edge effects, the model utilizes a periodic boundary in the x - and y -direction. For example, the periodic boundary condition implemented in the y -direction means that the node $(x, N_y - 1, z)$ is a nearest neighbour to the node at $(x, 0, z)$. Therefore, a particle going past the boundary on one side of the box results in the particle being wrapped back to the corresponding opposite side.

Cellular automata rules for bacterial behaviour. Cellular automata rules are used to update the occupation array, B , at each time step. The rules are locally applied to each

bacterium to determine its new state as a function of local environment and the previous state of that bacterium. The rules specify whether each bacterium divides, moves or detaches.

Let the parameter m_{avg} denote the average mass of an individual bacterium. For a bacterium to divide it must consume enough substrate to create a new daughter cell ($\approx m_{\text{avg}}/Y_{XS}$). Therefore, each bacterium, when created, is assigned a random 'division threshold' denoted by m_n , which is the cumulative mass of substrate needed for the bacterium to divide. The m_n value is drawn at random from the uniform distribution on the interval $[0.9 \times (m_{\text{avg}}/Y_{XS}), 1.1 \times (m_{\text{avg}}/Y_{XS})]$ (Evans *et al.*, 1993). Both m_n and the cumulative amount of substrate consumed by a bacterium to form biomass are stored in the I vector for that particular cell. Substrate consumption for each time increment is determined by multiplying (2) by the time step, Δt , and node volume, $27 \mu\text{m}^3$. The cumulative amount of substrate consumed by the bacterium increases until it exceeds m_n , in which case the cell divides. Any excess substrate consumed (above m_n) is kept with the parent bacterium as part of a new m_n for future division. (After completing these simulation experiments, we revised this rule to split the excess substrate equally between the parent and daughter cells. Direct comparison indicates that due to the relatively small excess of substrate left after cellular division there is no difference in population growth between the two rules).

The location (cube) of the newly created daughter cell is chosen at random from the 26 locations bordering the location of the mother cell (17 if the mother cell is on the substratum). If the selected cube is occupied, the daughter cell will displace cells in that direction until an empty cube is encountered. If the substratum or the original location (due to the periodic boundary conditions) is reached before encountering an empty volume element, a different daughter cell location is chosen at random.

In BacLAB, detachment is entirely governed by the local concentration of the detachment factor. Let the parameter $C_{F,\text{max}}$ denote a predetermined threshold concentration. Detachment occurs if and only if $C_F > C_{F,\text{max}}$ at the cell's location or if a cell is no longer anchored to the substratum due to other cells detaching. Three different detachment rules were investigated in a computer experiment. The first presumes removal of any bacterium at each node point that has reached the detachment factor threshold, $C_{F,\text{max}}$. This rule is referred to as local detachment. The second rule is similar to the first, but additionally removes any cell within a specified radius of detachment, R_d , of the node point where C_F exceeds $C_{F,\text{max}}$. This rule attempts to account for degradation of the extracellular polymeric substance as described by Boyd & Chakrabarty (1994). A hollowing of the biofilm structure is commonly observed with this detachment method, and it is therefore referred to as the hollow method. The third removal rule is similar to the second, with the exception that it also initiates the detachment of the plug or cylinder of biomass directly

above the hollowed region. These detached particles typically resemble cylinders and, therefore, this method is referred to as the cylinder method.

Computational steps. Fig. 1 shows the algorithm that defines BacLAB. The numbered steps in Fig. 1 correspond to the following sequence of operations. 1, Initialize the carrier surface with N_c randomly placed spherical colonies of radius R_c . Each cell within the colonies is itself inoculated with a random amount of substrate relative to division denoted by M , where M is chosen from a uniform $(0, m_n)$ distribution. 2, Generate the substrate distribution for the current time step, t , by finding the steady-state solution to (1). 3, Generate the detachment factor distribution for the current time step, t , by finding the steady-state solution to (1). 4, For each cube in Γ , determine if it is occupied by a bacterium. If the cube is unoccupied, nothing further is done with that volume element at the current time step. If the cube is occupied, further calculations are performed. 5, Each bacterium

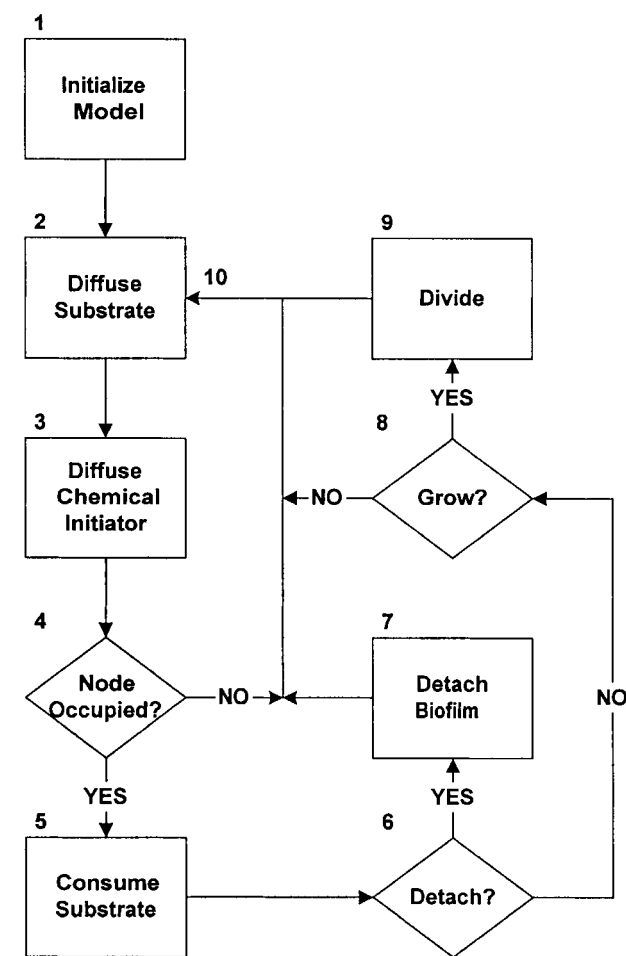


Fig. 1. General procedure followed in a typical simulation using BacLAB. See the 'Computational steps' section for an explanation of the sequence of operations.

consumes substrate based on (2) and the local concentration. The cumulative amount of substrate consumed for each cell, since its last division, is then updated. 6, Determine if C_F in the cube is above the detachment factor threshold, $C_{F,max}$. 7, Remove the bacterium in the current cube and any additional bacteria in other cubes according to the detachment rule specified. Additionally, identify and remove any floating clusters of bacteria. 8, Check if the bacterium has consumed enough substrate to divide. 9, Create a new bacterium neighbouring the parent and leave excess substrate (not required for the creation of a daughter cell) with the parent bacterium according to the rules specified. 10, Move forward in time by Δt based on the events that occurred in steps 4–9.

COMPUTER EXPERIMENT

Methods. Twenty replicate simulations, each for 500 time steps, were conducted for each detachment rule. Table 1 shows the values used to model the kinetics and solute transport for a typical bacterial biofilm. These representative values fit the ranges available from the literature, with the exception of those pertaining to the detachment factor, which had to be assumed. Each of the computer simulations began by inoculating a $300 \times 300 \mu\text{m}$ section of substratum with 28 randomly placed bacterial colonies (hemispheres) $30 \mu\text{m}$ in diameter as shown in Fig. 2(a). With the concentration of the substrate in the bulk fluid fixed at 20 mg l^{-1} , the simulation evolved in accordance to the set of rules discussed in the 'Computational steps' section.

At each time step, the program records the following response variables: cell areal density and biofilm thickness. Cell areal density is defined as the total number of cells in the model divided by the area and is given as cell per unit area of substratum (typically cm^2). The biofilm thickness is defined as the maximum height obtained by any single bacterium within the simulation. Thickness was measured this way to emulate measurements obtained with an optical microscope where a slide is removed from a reactor and placed on the microscope stage (Characklis, 1989). A $10 \times$ objective lens is then lowered until the top of the biofilm comes into focus and the fine adjustment dial setting is recorded. The objective is then lowered until the surface of the slide is in focus. The difference in the fine adjustment dial setting is then compared to a calibration curve to obtain the thickness.

Computational resources. BacLAB was written in C++ and compiled using the GCC compiler collection available from the Free Software Foundation. The differential equation solver, pois3d, was obtained as Fortran source code which was compiled and linked to BacLAB, again with the GCC compiler collection.

All experiments were performed on a dual 800 MHz Pentium III Mandrake Linux workstation with 1.5 gigabytes of PC133 SDRAM. A single experiment required approximately 700 megabytes of RAM. A simulation of 500 biofilm hours typically took about 8 computer hours. Although all experiments were conducted in a Linux/Unix environment, BacLAB has successfully been ported to a Microsoft Windows platform.

Analysis. The three-dimensional location data of each cell provide the ability to plot the biofilm in three-space and display the structural heterogeneity attained by BacLAB. Furthermore, by showing these images sequentially we are able to animate the structural development of the biofilm.

To visualize important quantitative characteristics for each simulation,

Table 1. Nomenclature, and kinetic and diffusion parameters used in the simulations

Parameter	Symbol	Value	Unit(s)
Spatial domain of the model	Γ		
Maximum specific growth rate	μ_{\max}	0.3125	h^{-1}
Time step	Δt	1	h
Identity pointer array	B		
Bulk detachment factor concentration	$C_{F,\text{bulk}}$	0	g m^{-3}
Detachment factor threshold	$C_{F,\text{max}}$	3.00×10^{-3}	g m^{-3}
Solute concentration	C_i		g m^{-3}
Bulk substrate concentration	$C_{S,\text{bulk}}$	20	g m^{-3}
Diffusivity of detachment factor in the aqueous phase (including the liquid, channels and voids)	$D_{F,\text{aq}}$	2.09×10^{-6}	$\text{m}^2 \text{h}^{-1}$
Relative effective diffusivity of detachment factor in biofilm	$D_{F,e}/D_{F,\text{aq}}$	0.30	
Diffusion coefficient of solute i	D_i		$\text{m}^2 \text{h}^{-1}$
Diffusion coefficient of solute i in aqueous phase	$D_{i,\text{aq}}$		$\text{m}^2 \text{h}^{-1}$
Relative effective diffusivity	$D_{i,e}/D_{i,\text{aq}}$		
Diffusivity of substrate in the aqueous phase (including the liquid, channels and voids)	$D_{S,\text{aq}}$	2.52×10^{-6}	$\text{m}^2 \text{h}^{-1}$
Relative effective diffusivity of substrate in biofilm	$D_{S,e}/D_{S,\text{aq}}$	0.45	
Detachment factor	F		
Detachment factor threshold	F_{\max}		g m^{-3}
Bacterium information array	I		
Detachment factor production coefficient	k	0.50	h^{-1}
Monod half-saturation coefficient	K_s	2.55	g m^{-3}
Average mass of an individual bacterium	m_{avg}	1.00×10^{-13}	g
Mass needed for division	m_n		g
Number of initial colonies	N_c	28	
Number of nodes in x -direction	N_x	300	
Number of nodes in y -direction	N_y	300	
Radius of initial colonies	R_c	15	μm
Radius of detachment	R_d	12	μm
Reaction rate of solute i	r_i		
Limiting substrate	S	Glucose	
Biomass density	X		g m^{-3}
Yield coefficient	Y_{XS}	0.45	$\text{g}_x \text{g}_S^{-1}$

we plot the biofilm thickness and cell areal density as functions of time. The geometric mean cell areal density and mean biofilm thickness of the 20 simulations were plotted at each time step for all detachment rules. For each detachment rule, an 80% envelope was constructed by sorting the 20 simulation values at each time step and plotting the third smallest and third largest values. This envelope provides an upper and a lower bound between which 80% of our data lie.

To quantitatively compare the different detachment rules, the mean \log_{10} (cell areal density) and mean biofilm thickness for each simulation were calculated in the transition and stationary phases, defined as 101–300 and 301–500 h, respectively. These times were chosen as oscillatory semi-steady values were observed after 300 h. Scatter plots of the means, \log_{10} (cell areal density) versus thickness, were created to see whether the data were clustered according to the detachment rule. Paired sample t -tests were then conducted to compare means between detachment rules.

RESULTS

Fig. 2(a–c) demonstrate the structural heterogeneity obtainable in BacLAB. An animation showing the dynamics of

the existing model is included as supplementary material in *Microbiology Online* (<http://mic.sgmjournals.org>). Fig. 2(a–c) were created by extracting three frames from such an animation. The key feature in these plots is the degree of structural heterogeneity created by the chemically initiated detachment mechanisms alone, in the absence of bulk fluid shear.

Fig. 3(a–c) present cell areal density data representing the 20 individual simulations for the local, hollow and cylinder rules, respectively, while Fig. 3(d–f) display the smoothed geometric mean and 80% envelope. Fig. 4 displays the biofilm thickness data in a similar manner. Because each simulation describes the biofilm characteristics on a 0.0081 cm^2 area of the surface, the cell areal density averaged over the 20 simulations corresponds to the areal density for a field of view of 0.162 cm^2 . The variation among the 20 simulations shows that different areas of the biofilm are not synchronized, but can grow and detach at different times.

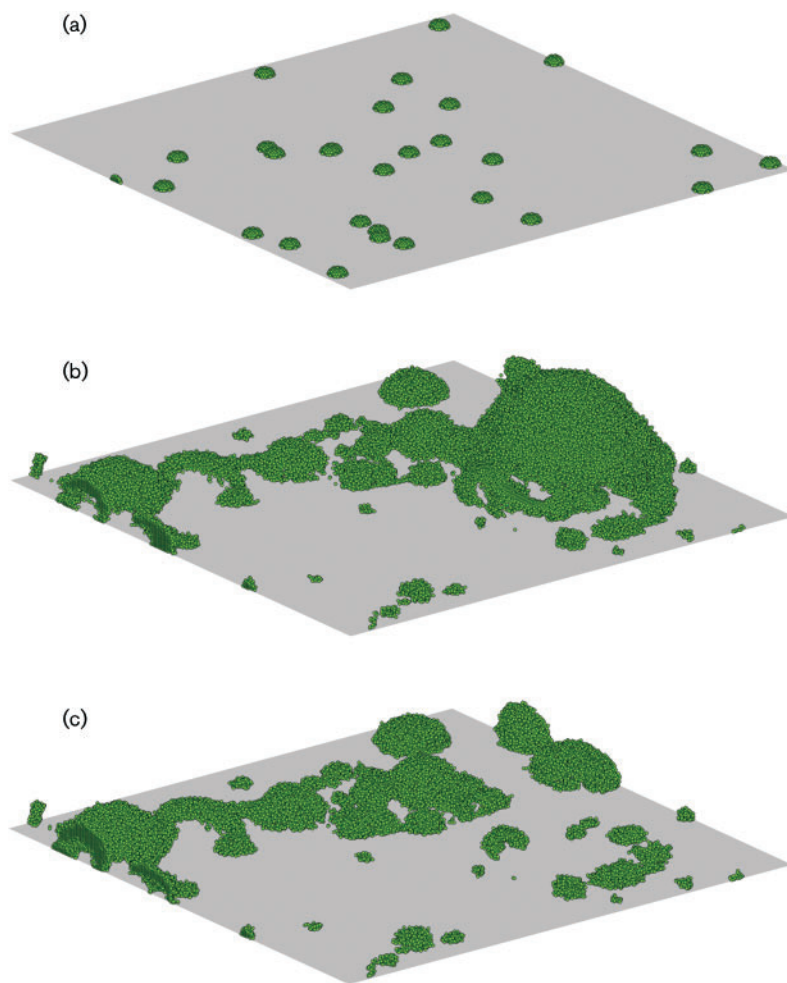


Fig. 2. Computer-simulated biofilm illustrating the biofilm (a) at the beginning of a simulation ($t=0$ h), (b) prior to a detachment event ($t=330$ h) and (c) following detachment ($t=335$ h). Data for constructing the biofilm images were saved every fifth time step (at 5 h intervals).

The cellular automata rules that govern the individual cells propagate into a consistent, but spatially variable, trend. The trends in Figs 3 and 4 are the exponential growth phase (0–100 h), followed by a relatively large sloughing event in the transition phase (101–300 h), followed by what appears to be an oscillatory ‘steady-state’ or stationary phase (301–500 h). These trends are observed for all three detachment rules to varying degrees. It should also be noted that the simulated cell areal densities are comparable to experimental densities found in the literature (Jackson *et al.*, 2001) for bacterial biofilms in general.

Fig. 5 demonstrates how the data are clustered by detachment rule in a plot of \log_{10} (cell areal density) versus biofilm thickness. Table 2 gives the mean and standard deviations of each characteristic for each detachment rule in the transition phase and stationary phase. All means within a given phase were statistically different ($P < 0.001$) with the exception of the cell areal density assuming hollow and cylinder rules ($P = 0.036$) and the biofilm thickness assuming local and hollow rules ($P = 0.052$) in the transition phase. On average, simulations with the local detachment rule result in a smaller cell areal density than does the hollow

rule which is smaller than the cylinder rule. For thickness, the order is reversed with the thickness using the local rule greater than biofilms which follow the hollow rule which is greater than biofilms which follow the cylinder rule. Low areal density and high thickness suggest a spatially heterogeneous biofilm. Therefore, due to the negative relationship between areal density and biofilm thickness in our simulations, the local rule leads to the roughest biofilm while the cylinder rule leads to the smoothest.

DISCUSSION

The goal of this research was to create a base model founded on well established transport equations that are easily adaptable to investigate conjectures at the biological level. The model does not incorporate all conventional biofilm development processes. Our model, BacLAB, controls biofilm development at the fundamental biofilm unit, the cell, and the resulting biofilm structure is produced by a process of self-organization. BacLAB with chemically induced detachment does create the typical heterogeneous ‘mushroom’ shape observed experimentally in biofilms. While it is beyond the scope of this report to investigate the detached

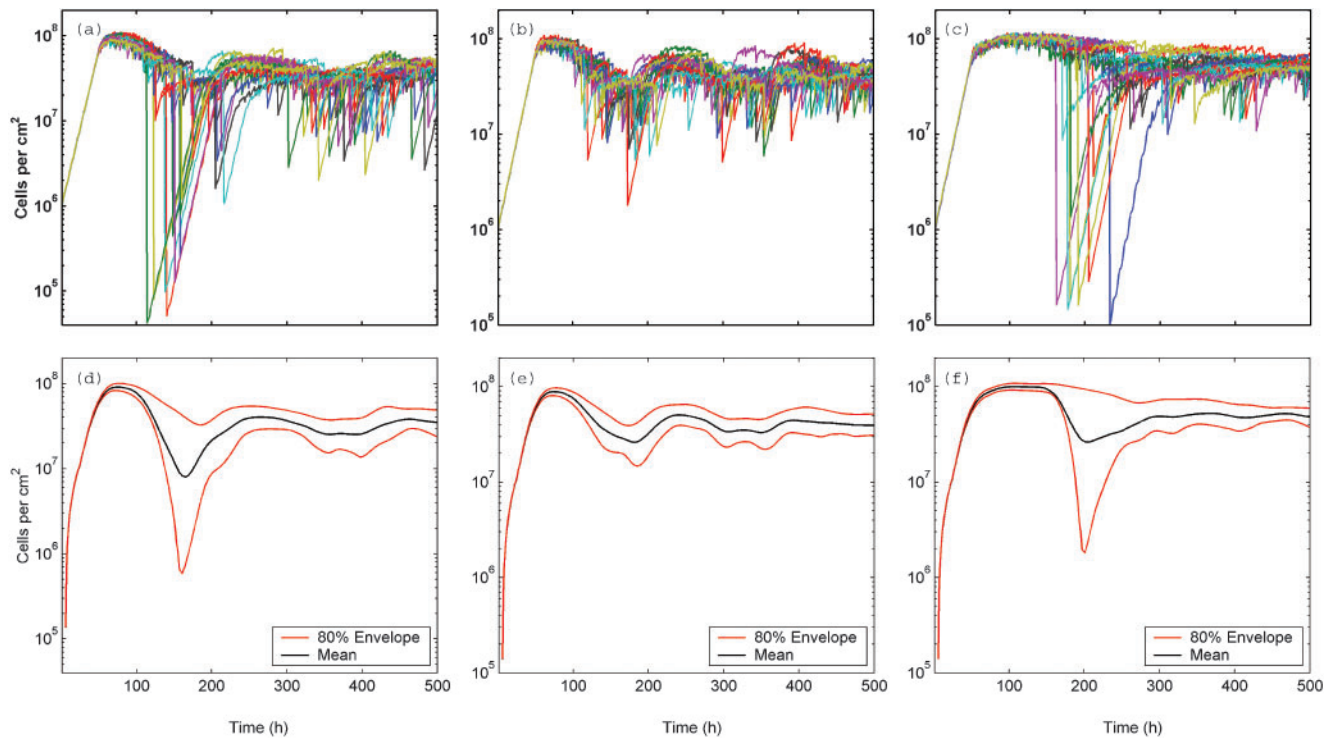


Fig. 3. Time series of the cell areal density data representing the 20 individual simulations for the (a) local, (b) hollow and (c) cylinder rules, respectively. Plots (d–f) show the smoothed geometric mean and 80 % envelope for plots (a–c), respectively, using a LOWESS smoother with 1 iteration and 0.1 as the smoother span.

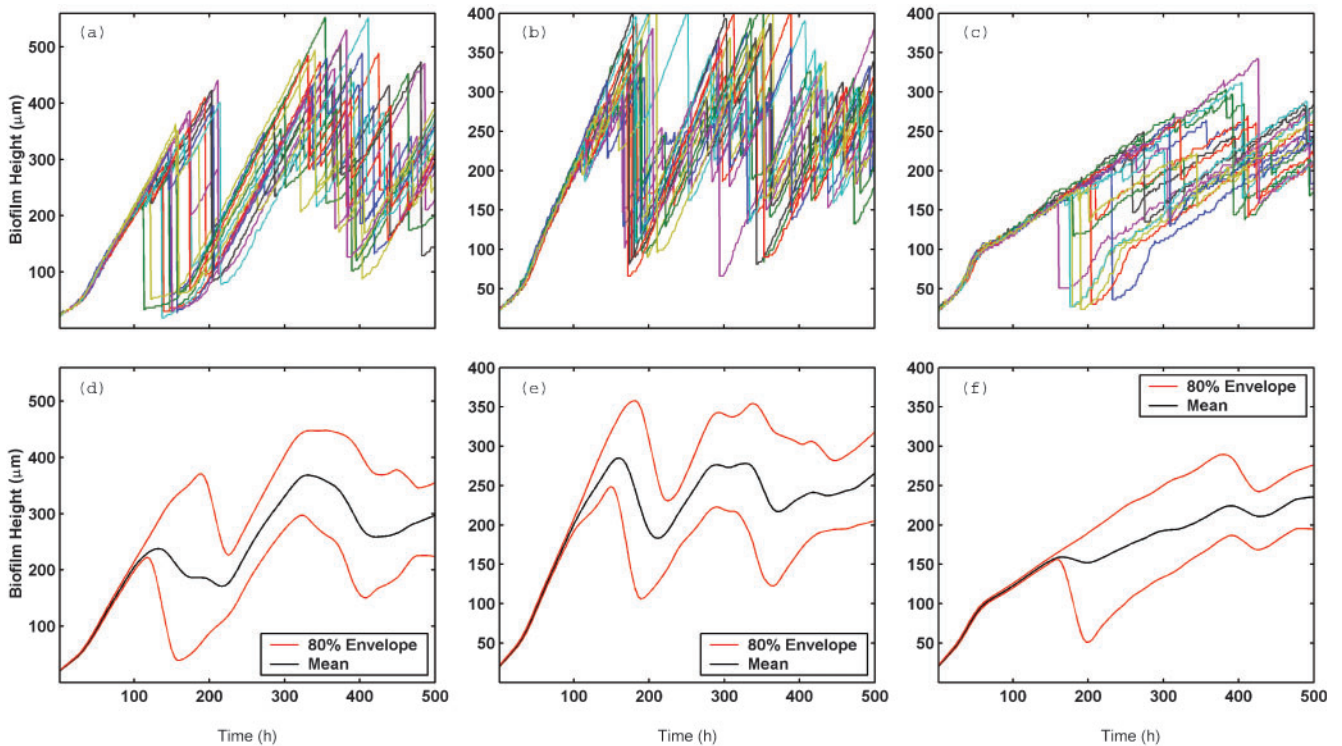


Fig. 4. Time series of the biofilm thickness data representing the 20 individual simulations for the (a) local, (b) hollow and (c) cylinder rules, respectively. Plots (d–f) show the smoothed arithmetic mean and 80 % envelope for plots (a–c), respectively, using a LOWESS smoother with 1 iteration and 0.1 as the smoother span.

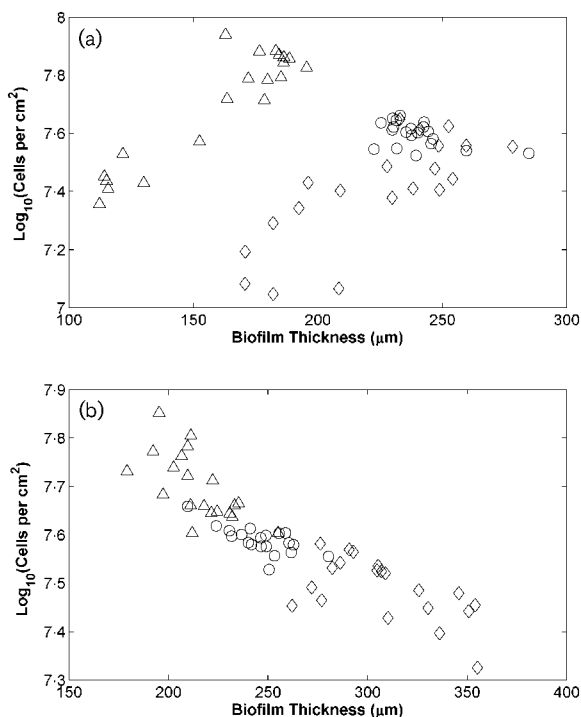


Fig. 5. Cell areal density (geometric mean) and mean biofilm thickness for each simulation in scatter plots for the (a) transition and (b) stationary phase. (a, b) \diamond , Local; \circ , hollow; \triangle , cylinder.

particle size distribution, it is clear that BacLAB predicts detached clumps ranging in size from a few bacteria to near complete removal of the biofilm. At first blush this appears to agree with observations made by Stoodley *et al.* (2001).

Modern biofilm research suggests that extracellular products play an important role in the development of biofilms. The BacLAB simulations assumed a chemical detachment factor accumulating locally leads to cellular detachment. Three rules were used to simulate the behaviour of this chemically mediated detachment. While these detachment

rules proved statistically different from one another, the differences are of little practical significance. The maximum difference in cell areal density between any two computer experiments in Fig. 5 is less than a log. Furthermore, the difference in biofilm thickness is difficult to interpret because it is a measurement of the most extreme point and, as such, highly variable (see Fig. 4). What we believe to be of practical significance is the observed trend (regardless of detachment rule) of a biofilm life cycle comparable to that observed in the laboratory. This life cycle begins when a carrier surface is inoculated with bacteria which undergo exponential growth until the biofilm reaches such a point that growth and detachment begin to offset one another. At this point the biofilm enters an oscillatory steady-state where the biofilm is maintained as a heterogeneous entity by constant growth and periodic detachment. If the detachment rule is removed from BacLAB, the simulated biofilm grows as an ever-thickening slab and no steady-state is reached.

We have examined one reasonable, growth-related theoretical explanation to the process of biofilm development by assuming a detachment mechanism in systems that impose no shear-stress on the biofilm. Conceivably, a combination of shear and normal forces induced by flowing bulk liquid also contributes to biofilm detachment. It is perhaps more plausible that chemical mediation and bulk fluid force acting in concert are responsible for the detachment of biofilms. The development of 'mushroom'-like biofilm clusters and interstitial voids and channels is typically thought to be a result of positive processes, like cell attachment, cell division and polymer production, and generally thought to result from some type of cellular organization. By refocusing on negative processes, such as cell detachment, we have shown that structures observed in real biofilms can be reproduced.

ACKNOWLEDGEMENTS

Support from the W. M. Keck Foundation and cooperative agreement EEC-8907039 between the National Science Foundation and Montana State University is gratefully acknowledged.

Table 2. Mean and standard deviation (SD) for the \log_{10} (cell areal density) and for biofilm thickness data in the transition and stationary phases for each detachment rule

Detachment rule	\log_{10} (cell areal density)				Biofilm thickness			
	Transition phase		Stationary phase		Transition phase		Stationary phase	
	Mean	SD	Mean	SD	Mean	SD	Mean	SD
Local	7.4	0.18	7.4	0.06	223	32.2	308	29.2
Hollow	7.5	0.04	7.5	0.02	239	13.6	246	15.6
Cylinder	7.6	0.19	7.6	0.06	160	30	215	17.6

REFERENCES

- Allison, D. G., Heys, S. J. D., Willcock, L., Holah, J. & Gilbert, P. (1999). Cellular detachment and dispersal from bacterial biofilms: a role for quorum sensing? In *Biofilms: the Good, the Bad and the Ugly*, pp. 279–286. Edited by J. Wimpenny, P. Gilbert, J. Walker, M. Brading & R. Bayston. Cardiff, UK: Bioline.
- Barker, G. C. & Grimson, M. J. (1993). A cellular automaton model of microbial growth. *Binary* 5, 132–137.
- Boyd, A. & Chakrabarty, A. M. (1994). Role of alginate lyase in cell detachment of *Pseudomonas aeruginosa*. *Appl Environ Microbiol* 60, 2355–2359.
- Characklis, W. G. (1989). *Biofilms*, pp. 55–89, p. 114. Edited by W. G. Characklis & K. C. Marshall. New York: Wiley.
- Colasanti, R. L. (1992). Cellular automata models of microbial colonies. *Binary* 4, 191–193.
- Davies, D. G., Parsek, M. R., Pearson, J. P., Iglewski, B. H., Costerton, J. W. & Greenberg, E. P. (1998). The involvement of cell-to-cell signals in the development of a bacterial biofilm. *Science* 280, 295–298.
- Eberl, H. J., Picioareanu, C., Heijnen, J. J. & van Loosdrecht, M. C. M. (2000). A three-dimensional numerical study on the correlation of spatial structure, hydrodynamic conditions, and mass transfer and conversion in biofilms. *Chem Eng Sci* 55, 6209–6222.
- Ermentrout, G. B. & Edelstein-Keshet, L. (1993). Cellular automata approaches to biological modeling. *J Theor Biol* 160, 97–133.
- Evans, M., Hastings, N. & Peacock, B. (1993). Rectangular (uniform) continuous distribution. In *Statistical Distributions*, pp. 137–140. New York: Wiley.
- Hermanowicz, S. W. (1998). Model of two-dimensional biofilm morphology. *Water Sci Technol* 37, 219–222.
- Hermanowicz, S. W. (1999). Two-dimensional simulations of biofilm development: effects of external environmental conditions. *Water Sci Technol* 39, 107–114.
- Jackson, G., Beyenal, H., Rees, W. M. & Lewandowski, Z. (2001). Growing reproducible biofilms with respect to structure and viable cell counts. *J Microbiol Methods* 37, 1–10.
- Kolter, R. & Losick, R. (1998). One for all and all for one. *Science* 280, 226–227.
- Kreft, J. U., Booth, G. & Wimpenny, J. W. T. (1998). BacSim, a simulator for individual-based modelling of bacterial colony growth. *Microbiology* 144, 3275–3287.
- Monod, J. (1949). The growth of bacterial cultures. *Annu Rev Microbiol* 3, 371–394.
- Noguera, D. R., Pizarro, G., Stahl, D. A. & Rittmann, B. E. (1999). Simulation of multispecies biofilm development in three dimensions. *Water Sci Technol* 39, 123–130.
- Picioareanu, C., van Loosdrecht, M. C. M. & Heijnen, J. J. (1998). A new combined differential-discrete cellular automaton approach for biofilm modeling: application for growth in gel beads. *Biotechnol Bioeng* 57, 718–731.
- Picioareanu, C., van Loosdrecht, M. C. M. & Heijnen, J. J. (1999). Discrete-differential modeling of biofilm structure. *Water Sci Technol* 39, 115–122.
- Potera, C. (1999). Forging a link between biofilms and disease. *Science* 283, 1837–1839.
- Rittmann, B. E. & Manem, J. A. (1992). Development and experimental evaluation of a steady-state, multispecies biofilm model. *Biotechnol Bioeng* 39, 914–922.
- Rittmann, B. E. & McCarty, P. L. (1980). Model of steady-state-biofilm kinetics. *Biotechnol Bioeng* 22, 2343–2357.
- Sauer, K., Camper, A. K., Ehrlich, G. D., Costerton, J. W. & Davies, D. G. (2002). *Pseudomonas aeruginosa* displays multiple phenotypes during development as a biofilm. *J Bacteriol* 184, 1140–1154.
- Stewart, P. S., Peyton, B. M., Drury, W. J. & Murga, R. (1994). Quantitative observations of heterogeneities in *Pseudomonas aeruginosa* biofilms. *Appl Environ Microbiol* 59, 327–329.
- Stoodley, P., Wilson, S., Hall-Stoodley, L., Boyle, J. D., Lappin-Scott, H. M. & Costerton, J. W. (2001). Growth and detachment of cell clusters from mature mixed species biofilms. *Appl Environ Microbiol* 67, 5608–5613.
- Wanner, O. & Gujer, W. (1986). Multispecies biofilm model. *Biotechnol Bioeng* 28, 314–328.
- Wanner, O. & Reichert, P. (1996). Mathematical modeling of mixed-culture biofilms. *Biotechnol Bioeng* 49, 172–184.
- Watnick, P. & Kolter, R. (2000). Biofilm, city of microbes. *J Bacteriol* 182, 2672–2679.
- Wimpenny, J. W. T. & Colasanti, R. (1997). A unifying hypothesis for the structure of microbial biofilms based on cellular automaton models. *FEMS Microb Ecol* 22, 1–16.